Pergamon

Bioorganic & Medicinal Chemistry 9 (2001) 2589–2600

BIOORGANIC & MEDICINAL CHEMISTRY

Characterization of a DNA-Cleaving Deoxyribozyme

Nir Carmi and Ronald R. Breaker*

Department of Molecular, Cellular and Developmental Biology, Yale University, New Haven, CT 06520-8103, USA

Received 17 November 2000; accepted 2 January 2001

Abstract—A copper-dependent self-cleaving DNA that was isolated by in vitro selection has been minimized to its smallest active domain using both in vitro selection and rational design methods. The minimized 46-nucleotide deoxyribozyme forms duplex and triplex substructures that flank a highly conserved catalytic core. This self-cleaving construct can be converted into a bimolecular complex that comprises separate substrate and enzyme domains. Substrate cleavage is directed at one of two adjacent nucleotides and proceeds via an oxidative cleavage mechanism that is unique to the position cleaved. The structural, kinetic and mechanistic characteristics of this DNA-cleaving deoxyribozyme are reported. © 2001 Published by Elsevier Science Ltd.

Introduction

Single-stranded DNA can fold into complex tertiary structures and play an active role in molecular recognition[1–4] and catalysis.[5–8] Although DNA serves primarily a genetic role in nature, single-stranded DNAs can be engineered to perform a number of catalytic tasks that are typically reserved for biopolymers made of protein or RNA.[9] Each of these deoxyribozymes has been isolated from a random-sequence population of DNA by using in vitro selection.[10] This combinatorial strategy has been used to create numerous classes of RNA-cleaving deoxyribozymes,[11–18] some of which hold promise as useful agents for the targeted destruction of RNA inside cells.[19–25]

Similarly, DNAs that catalyze the cleavage of DNA could be used to target other DNA molecules for destruction, or for designing DNA constructs that self-process. However, engineering deoxyribozymes that hydrolyze DNA is expected to be very challenging. By comparison, each class of RNA-cleaving deoxyribozymes catalyzes cleavage of the RNA 3′,5′-phosphodiester linkage by promoting an internal transesterification reaction to produce 2′,3′-cyclic phosphate and 5′-hydroxyl termini. The uncatalyzed rate of RNA transesterification proceeds ~100,000-fold faster than the uncatalyzed rate for the related hydrolytic DNA cleavage reaction.[26] This difference in chemical stability is caused by RNA's 2′-hydroxyl group, which serves as a pre-positioned nucleophile for attack at the adjacent phosphorus center. As a result, deoxyribozymes that rapidly hydrolyze DNA must form an active site that can bind and position water as a nucleophile. This extra mechanistic requirement is likely to demand greater complexity in DNA structure relative to those formed by RNA-cleaving deoxyribozymes. Alternatively, deoxyribozymes can promote DNA strand scission by other catalytic mechanisms. For example, a self-cleaving *N*-glycosylase deoxyribozyme was isolated recently that catalyzes the site-specific depurination of a particular deoxyguanosine residue.[27] A spontaneous β-elimination reaction at the depurinated site results in DNA chain cleavage.

We have isolated a series of Cu^{2+}-dependent self-cleaving DNAs by in vitro selection that catalyze the oxidative cleavage of DNA.[28,29] Individual DNA molecules undergo self-cleavage in the presence of the cofactors Cu^{2+} and ascorbate. Hydroxyl radicals are produced by the oxidation of ascorbate and the subsequent reduction of dioxygen, in a transition metal-catalyzed sequence of reactions, to produce hydrogen peroxide and dehydroascorbate.[30] In the subsequent Fenton-like reaction, each H_2O_2 molecule is further reduced to generate a hydroxyl ion and a hydroxyl radical via a reaction that

*Corresponding author. Tel.: +1-203-432-9389; fax: +1-203-432-5713; e-mail: ronald.breaker@yale.edu

0968-0896/01/$ - see front matter © 2001 Published by Elsevier Science Ltd.
PII: S0968-0896(01)00035-9

is also catalyzed by a redox-active metal. Hydroxyl radicals can diffuse freely in solution and can cause the non-specific cleavage of both nucleic acids and proteins.[31] The oxidative modification of DNA by hydroxyl radicals can take place at various positions on the base or deoxyribose moieties.[32] Specifically, oxidation at the C1′, C4′, or C5′ positions of deoxyribose induce chemical rearrangements that result in polynucleotide chain cleavage.[33] Random cleavage of DNA is readily observable upon incubation of polynucleotides in the presence of millimolar concentrations of mono- or divalent copper when combined with a similar concentration of ascorbate.[28] Several DNA-cleaving agents such as 1,10-phenanthroline dramatically enhance the rate of DNA cleavage by Cu^{2+} and ascorbate, even when both Cu^{2+} and the DNA-cleaving agent are used at micromolar concentrations.[34] Supplementing these oxidative cleavage reactions with H_2O_2 produces even greater rates of DNA chain cleavage, while enzymatically removing H_2O_2 from the reaction using catalase prevents the cleavage of DNA.[35]

The self-cleaving deoxyribozymes that we have isolated by in vitro selection greatly accelerate the oxidative cleavage of DNA in the presence of nanomolar concentrations of Cu^{2+}. Two distinct classes of Cu^{2+}-dependent deoxyribozymes (I and II) were isolated from the selected population. Class I self-cleaving DNAs require the presence of both Cu^{2+} and ascorbate for catalytic function,[28] and presumably employ a cleavage mechanism that is analogous to those that result in the non-specific DNA cleavage when very high concentrations of these cofactors are used. DNA cleavage by class I molecules is focused in a single region near the 5′ terminus of the molecule, which indicates that the self-cleaving DNA forms an active site that confers spatial organization to an otherwise random oxidative cleavage process.

Class II deoxyribozymes catalyze Cu^{2+}-dependent self-cleavage in the absence of ascorbate, albeit with a catalytic rate that is only 1/2000th that of the corresponding rate in the presence of both Cu^{2+} and ascorbate (k_{obs} min^{-1} at Clv1 $= 8\times10^{-4}$ and 1.4×10^{-1} for either one or both cofactors, respectively).[28] This class can undergo self-cleavage in two distinct regions (Clv1 and Clv2), suggesting that two regions of the DNA chain might come in close proximity to the active site. Further optimization of the DNA-cleaving activity of class II deoxyribozymes provided variants with catalytic rates that are improved by greater than 50-fold in the presence of Cu^{2+} as the only cofactor. This activity is surprising, because oxidative damage to DNA is not observed under similar treatments with redox-active metal ions such as Fe^{3+} or Cu^{2+} when incubated in the absence of added ascorbate, or even when alternative reducing agents such as dithiothreitol or glutathione are used.[31] Recently, we reported the minimization of class II self-cleaving DNAs and their conversion into a more generalizable 'restriction enzyme' for use in cleaving single-stranded DNA substrates.[29] Herein, we describe the structural, kinetic and mechanistic characteristics of this novel class of Cu^{2+}-dependent DNA-cleaving deoxyribozymes.

Results

A minimized domain for class II DNA-cleaving deoxyribozymes

The smallest self-cleaving domain that was obtained through in vitro selection was 69 nucleotides in length. The predicted secondary structure for this class of deoxyribozymes includes two stem-loops (I and II) that are interspersed with three single-stranded domains. In addition, a contiguous series of 21 nucleotides comprising the 3′ terminus of variant self-cleaving DNAs remained highly conserved throughout the in vitro selection process, indicating that these nucleotides were critical for deoxyribozyme function.[28] We have used this information to design a 46-nucleotide self-cleaving DNA (Fig. 1) that retains this conserved sequence domain. Specifically, 26 nucleotides of the original 69mer DNA were replaced with a DNA 'triloop' that has been shown to enhance the stability of adjoining stem structures.[36] The 46mer undergoes Cu^{2+}-dependent self-cleavage with a rate that matches that of the original full-length deoxyribozyme (k_{obs} of $\sim0.3\,min^{-1}$).

The 46mer can be divided into separate substrate and catalyst domains that are represented, for example, by the synthetic oligonucleotides s1 (substrate) and c1 (catalyst) as depicted in Figure 2(a). The substrate DNA includes the primary site of DNA cleavage, while the

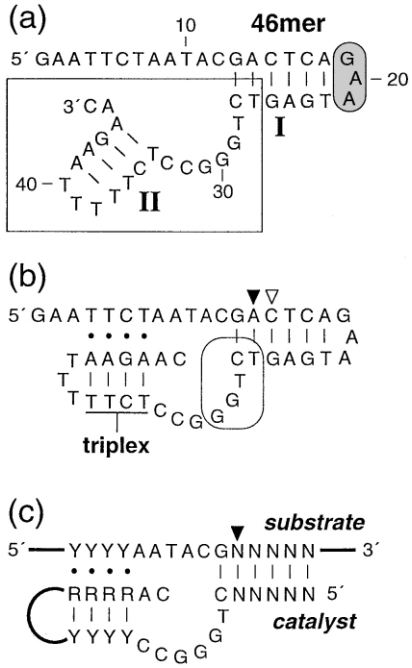

Figure 1. Class II DNA-cleaving deoxyribozymes. (a) Sequence and pistol-like secondary structure of a 46-nucleotide self-cleaving DNA. **I** and **II** designate putative stem-loop structures (lines indicate Watson–Crick base pairs). Boxed nucleotides were highly conserved during the in vitro selection process.[28,29] Shaded nucleotides can be deleted to create a bimolecular arrangement. (b) Duplex and triplex interactions between substrate and catalyst domains. Triplex interactions are represented by dots. The filled and open triangles, respectively, identify the major and minor sites of DNA cleavage in the substrate domain. Encircled nucleotides identify the region of the catalyst that also is susceptible to Cu^{2+}-dependent cleavage. (c) Consensus sequence for cleaving substrate DNAs with engineered class II catalysts. R, Y and N represent purine, pyrimidine and any nucleotide, respectively.

catalyst DNA contains the original random-sequence domain that also contains all the nucleotides that were conserved during the in vitro selection process. The 18-nucleotide s1 and 25-nucleotide c1 DNAs do not undergo self-cleavage when tested individually under the permissive reaction conditions. However when mixed, these DNAs form a bimolecular complex that retains full catalytic activity (Fig. 2b; lane 1) (k_{obs} $\sim$0.15 min^{-1} for s1 cleavage).

To examine whether the catalyst strand could be further truncated at the 3′ terminus, we synthesized and tested the oligonucleotide c1-C (Fig. 2a). This DNA is identical to c1 except that the 3′-terminal cytosine residue was not included during chemical preparation. Unlike c1, the c1-C oligomer is not able to cleave s1 when incubated in reaction buffer A (see Experimental) containing 10 μM Cu^{2+} (Fig. 2b; lane 2). Interestingly, c1-C can cleave s1 when the reaction mixture is supplemented with 10 μM of either L-ascorbate or D-isoascorbic acid, or when H_2O_2 is added to the reaction mixture (Fig. 2b; lanes 3–5, respectively). These results indicate that the 3′-terminal C residue of c1 is critical for ascorbate-independent activity, and that the role served by this nucleotide can be at least partially fulfilled by the addition of a reducing agent or H_2O_2.

Evidence for the secondary-structure model of class II deoxyribozymes

The predicted secondary structure of the minimized 46mer DNA (Fig. 1a) consists of two stem-loops (I and II) that are interspersed with three single-stranded domains. This secondary structure is supported by mutational analysis of the putative pairing regions. For example, altering the nucleotide sequence of the catalyst DNA within stem I created an altered substrate specificity for DNA cleavage.[29] Although stem I formation is important for deoxyribozyme function, the sequences that comprise this structural element can be varied as long as base complementation is retained (Fig. 1c).

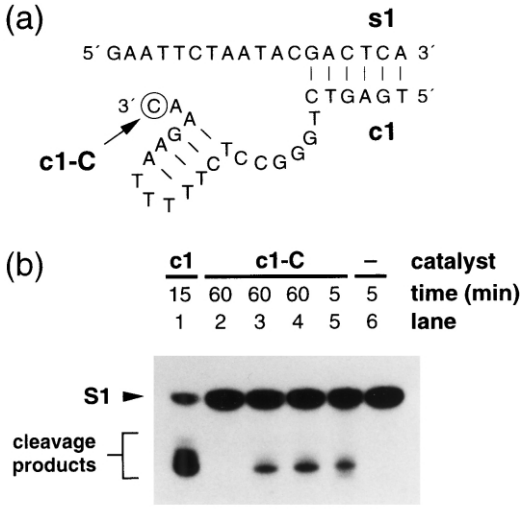

Figure 2. Structural model and sequences for bimolecular DNA complexes. (a) A bimolecular complex can be constructed by uncoupling the 46mer self-cleaving DNA via removal of the three-nucleotide loop of stem I, thereby creating separate DNA strands that are designated as 's' and 'c' oligomers. The complex comprised of s1 and c1 DNAs constitute a minimal catalytic structure. Oligomer c1-C is created by deletion of the 3′-terminal nucleotide of c1 (encircled). (b) Cleavage of DNA by c1 and c1-C in buffer A (see Experimental) containing 30 μM $CuCl_2$. Trace amounts of 5′ ^{32}P-labeled s1 were incubated with 5 μM c1, 5 μM c1–C, or in the absence (–) of catalyst DNA. In addition, lanes 3, 4 and 5 contain 10 μM L-ascorbate (sodium form), 10 μM D-isoascorbic acid or 35 mM H_2O_2, respectively. Reaction products were separated by denaturing 20% PAGE and imaged by autoradiography.

In addition, the affinity of the deoxyribozyme for its corresponding substrate is dictated by the overall strength of stem I base pairing. Extension of stem I from six base pairs to 10 base pairs yields a deoxyribozyme that exhibits a marked improvement in substrate affinity. We compared the concentration-dependent activities of catalyst c1 (Fig. 2a) with catalyst c4 (Fig. 3a) using trace amounts of 5′ ^{32}P-labeled substrate s4. Both c1 and c4 cleave the extended s4 oligomer with comparable yields when micromolar concentrations of catalyst are used (Fig. 3b). However, only the activity of c4 can be detected when sub-nanomolar concentrations of catalyst are used. This observation is consistent with the view that complex formation is driven, at least in part, by base pairing interactions between the complementary stem I elements of substrate and catalyst DNAs.

Similarly, we examined various deoxyribozyme mutants to examine two different but equally plausible base pairing interactions that would form stem II (Fig. 4a). Contact *i* is a hypothetical stretch of four base pairs that can be formed between the substrate and catalyst domains. In most RNA-cleaving ribozymes and deoxyribozymes, the cleavage site resides in a bulged structure that is flanked on both sides by base-paired regions. Contact *i* would produce this more conventional

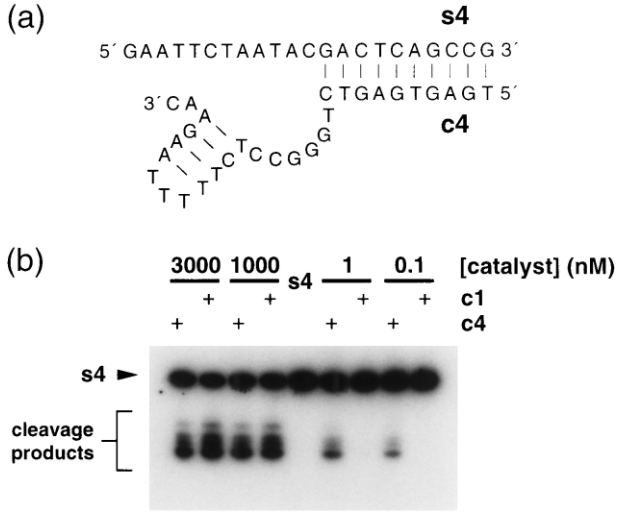

Figure 3. . Concentration-dependent activity of catalyst DNAs that carry different-sized stem I domains. (a) Secondary-structure model of the complex formed between s4 and c4 DNAs. (b) Trace amounts of 5′ ^{32}P-labeled s4 were incubated at 23 °C for 15 min (3000 and 1000 nM catalyst DNA) or for 2 and 4 h (1 and 0.1 nM catalyst DNA, respectively) in a reaction mixture containing buffer A plus 30 μM $CuCl_2$. Lane identified as s4 contains labeled s4 DNA as a marker. Reaction products were separated by denaturing 20% PAGE and imaged by autoradiography.

secondary-structure motif for class II deoxyribozymes. In contrast, contact *ii* can be formed with nucleotides that reside entirely within the conserved domain of the catalyst strand. Formation of *ii* would create a hairpin that produces the pistol-like secondary structure (Fig. 1a) that is predicted by the Zuker DNA MFOLD program.* To initiate our assessment of the two structural possibilities, we synthesized a substrate oligonucleotide (s1-GAA) in which the three 5′-terminal nucleotides of s1 are deleted. The truncated substrate is cleaved with drastically reduced efficiency when incubated with c1 (Fig. 4c). As a result, further deletion of the substrate DNA could not be carried out in order to assess the impact on deoxyribozyme activity upon removal of the contact *i* pairing element within the substrate molecule. However, mutations within the possible base-pairing region of *i* eliminate catalytic activity, even when compensatory changes are made that are expected to restore base pairing (Fig. 4b and c). This, coupled with the fact that both the 5′-terminal GAA and the 3′-terminal C residues on the substrate and catalyst domains, respectively, are required for full activity indicate that contact *i* is not important for catalytic function.

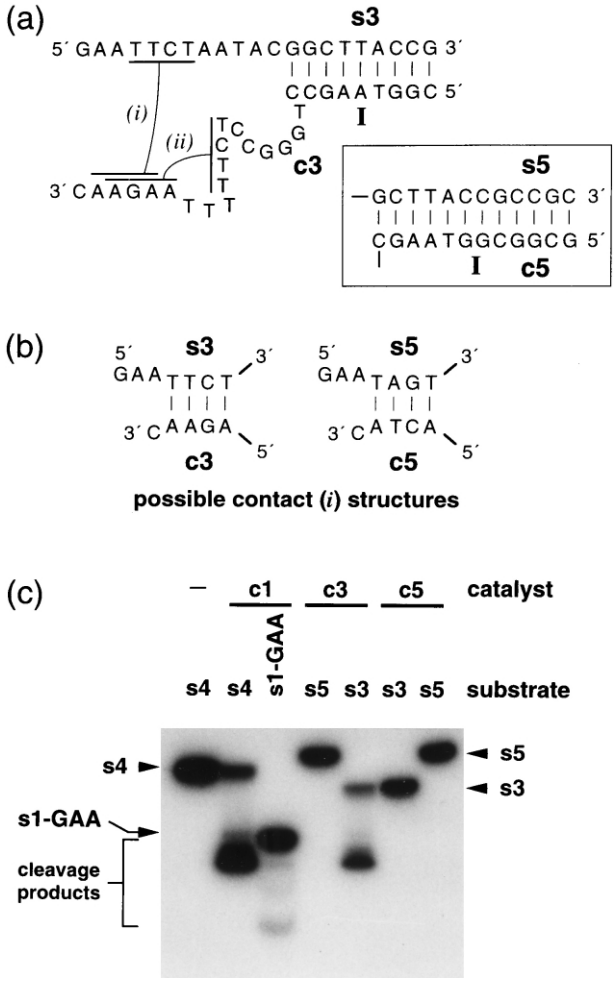

Figure 4. Analysis of possible stem II arrangements. (a) Two regions of base complementation are identified as 'contact *i*' and 'contact *ii*'. Inset provides the stem I sequences for s5 and c5. (b) Sequence changes made to assess the validity of contact *i*. (c) DNA cleavage assays used to assess the validity of proposed contact *i*. Trace amounts of 5′ ^{32}P-labeled substrate as indicated were incubated with 5 μM catalyst DNA also as indicated in buffer A containing 30 μM $CuCl_2$ at 23 °C for 15 min. Reaction products were separated by denaturing 20% PAGE and imaged by autoradiography.

*The DNA MFOLD algorithm can be accessed on the internet (http://bioinfo.math.rpi.edu/~mfold/dna/form1.cgi).

In contrast, variant 46mer deoxyribozymes with mutations that affect contact *ii* display activities that are consistent with the presence of a stem-loop structure (stem II) as shown in Figure 1(a). As previously demonstrated,[29] disruption of the C35–G43 base pair in putative stem II, either by a C to G mutation at position 35 or the corresponding G to C mutation at position 43, results is a drastic loss of deoxyribozyme activity. DNA cleavage activity is partially restored when these mutations are combined in the same molecule to produce a G35–C43 base pair. Furthermore, mutations that are consistent with contact *ii* and its involvement in a DNA triplex structure with the substrate (Fig. 1b) can be used to alter the substrate specificity of class II deoxyribozymes.[29] Finally, the presence of a triplex element involving stem II is supported by NMR analysis and thermal melting data (N. Carmi, R. Baliga, D. M. Crothers and R. R. Breaker, unpublished observations). This structural arrangement results in the localization of the two cleavage regions of class II in close proximity to the base of stem I (Fig. 1b).

Additional support for the participation of contact *ii* in the active class II structure was found upon examination of the in vitro selected DNAs. A single self-cleaving DNA that was isolated after 13 rounds of selection,[28] (data not shown) carries a core sequence that differs significantly from the remaining individual DNAs that were isolated from the same DNA pool. As with the 46mer, the variant DNA was divided into separate substrate and catalyst domains (Fig. 5) and the oligonucleotides were combined to assess catalytic activity. The synthetic oligonucleotide c6 cleaves s1 with a rate constant that is 10% of that exhibited by c1, despite the fact that c6 differs significantly from c1 in the conserved-sequence domain. The variant bases found in c6 either are seen in other class II deoxyribozymes (C to T base change at position 11), or are consistent with a stem-loop structure formed by contact *ii*. These findings support the model for class II deoxyribozymes wherein the DNA forms duplex and triplex structures (Fig. 1b).[29] In a bimolecular format, these structures act independently as substrate-binding domains, and can be engineered to cleave single-stranded DNA at specific positions along the polynucleotide chain (Fig. 1c).

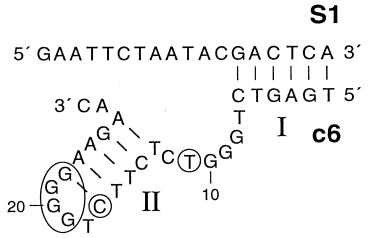

Figure 5. Sequence and secondary structure of a variant class II deoxyribozyme that was isolated by in vitro selection. Encircled nucleotides vary from that of the otherwise conserved sequences of the original 46mer DNA.

Requirements for optimal deoxyribozyme function

The 46mer exhibits a narrow functional range for temperature, with an optimum activity reached at 23 °C. This temperature-dependent functional range can be broadened by elongating stem II with concomitant extension of the triplex domain (data not shown). The activity of the 46mer also is highly dependent on the concentration of monovalent cations (Fig. 6a), which presumably serve to stabilize the active conformation of the deoxyribozyme. Although in vitro selection was carried out in the presence of both NaCl and KCl (0.5 M each), we find that both Na^+ and K^+ can serve independently as the form of monovalent cation with almost equal efficiency. Both cations produce maximum deoxyribozyme activity at a concentration of approximately 0.3 M.

Deoxyribozyme function is also sensitive to pH (Fig. 6b). Maximal activity is attained at pH 7.0, which corresponds to the pH of the buffer A, which was used during the in vitro selection process.[28] However, the deoxyribozyme remains measurably active at extreme pH values. For example, DNA self-cleavage proceeds with a k_{obs} of $\sim 10^{-2}\,min^{-1}$ at pH 4.0 (data not shown). It is known that the stability of YR*Y triple helices that contain CG*C^+ base triples can be sensitive to pH. This results from the fact that each cytosine residue in the third strand of the triplex requires protonation of N3 to stabilize its interaction with the Hoogsteen face of the paired guanosine nucleotide.[37,38] The pK_a of the N3 of cytidine-5′ phosphate is 4.54,[39,40], and triplex interactions that make extensive use of CG*C^+ base triples are destabilized by higher pH values.[41] We have tested a variant deoxyribozyme in which the CG*C^+ triple is replaced with a TA*T triple. The variant deoxyribozyme remains fully active, but shows no significant difference in pH-dependent activity compared to a construct with the original triplex sequence (Fig. 2b). This indicates that the deoxyribozyme's sensitivity to reaction mixtures with relatively high pH is not due to destabilization of the triplex motif.

The rate of DNA cleavage is highly dependent on the concentration of divalent copper that is used in the reaction mixture. The 46mer has an apparent K_d for Cu^{2+} of ~300 nM, and displays maximal activity near 10 μM (Fig. 6c). The deoxyribozyme is severely inhibited at concentrations in excess of 100 μM Cu^{2+}. Another Cu^{2+}-dependent deoxyribozyme with DNA ligase activity ([Cu^{2+}] optimum = 10 μM) has been shown to experience a similar inhibitory effect with higher metal ion concentrations.[42] It is known that high concentrations of Cu^{2+} (> 100 μM) causes the disruption of single- and double-stranded nucleic acid structures.[43] We speculate that the inhibitory effect of high copper concentrations in our assays could be due to a similar mechanism, whereby the non-specific binding of Cu^{2+} to DNA disrupts deoxyribozyme structure and function.

To examine this possibility, we conducted a series of deoxyribozyme assays with s1 and c1 wherein either the total DNA concentration or the total Cu^{2+} concentration was varied. We find that increasing the concentration of c1 does not lead to progressively higher cleavage rates or even to a rate plateau, but that relatively high concentrations of c1 DNA inhibit the DNA cleavage reaction (data not shown). This inhibitory effect is not dependent on the sequence of DNA that is added, since other DNAs with sequences that are unrelated to s1 or c1 also inhibit deoxyribozyme function when present in micromolar concentrations. We also find that this inhibitory effect loosely correlates with the mole equivalents of nucleotide that are added. Furthermore, the inhibitory effect of DNA addition can be offset by increasing the concentration of Cu^{2+} in the reaction mixture. These findings are consistent with the possibility that Cu^{2+} binds to DNA non-specifically with K_d values that are in the micromolar range. The loss of DNA cleavage activity, therefore, might be due to a deficit of free metal cofactor, as Cu^{2+} becomes sequestered from the active site of the catalysts due to non-specific binding with excess DNA molecules.

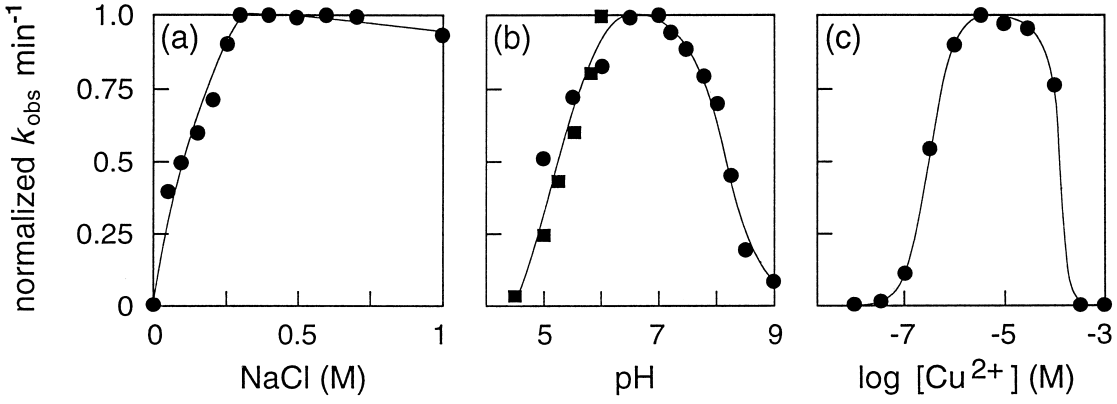

Figure 6. Kinetic characteristics of the 46mer self-cleaving DNA. All reactions were conducted using trace amounts of 5′ ^{32}P-labeled 46mer DNA in 50 mM HEPES. (a) Reactions containing variable NaCl concentration were conducted at pH 7, 23 °C with 30 μM $CuCl_2$. (b) Reactions conducted under different pH conditions contained 0.5 M NaCl, 30 μM $CuCl_2$, and were incubated at 23 °C. (c) The effect of Cu^{2+} concentration on deoxyribozyme function was assessed with cleavage assays conducted as described in (a), except that 0.5 M NaCl was present and the $CuCl_2$ concentration was varied from 10 nM to 1 mM.

DNA cleavage sites and reaction products

Enrichment or depletion of oxygen in the reaction solution enhances or diminishes catalytic rate, respectively (data not shown). Moreover, the introduction of catalase (bovine liver) to a final concentration of 0.3 U/μL prevents deoxyribozyme function, while the addition of hydrogen peroxide induces the deoxyribozyme to function with a rate constant that exceeds that observed with Cu^{2+} alone. These results are consistent with an oxidative cleavage mechanism that makes use of molecular oxygen and hydrogen peroxide for the cleavage of DNA. We have conducted a more detailed characterization of the DNA cleavage products in order to assess the results of this oxidative cleavage process.

High-resolution PAGE was used to more carefully define the sites of Cu^{2+}-dependent DNA cleavage catalyzed by class II deoxyribozymes. The use of 5′ ^{32}P-labeled substrate or catalyst DNAs reveals that each undergoes cleavage at several closely-grouped sites. Four distinct product bands are evident upon cleavage of 5′ ^{32}P-labeled s4 DNA by c4 (Fig. 7a). The major substrate cleavage product has a gel mobility that is slightly slower than a synthetic DNA marker that consists of the first 12 nucleotides of the substrate. The slower mobility of the major cleavage product indicates that this DNA could be a 13-nucleotide product that carries a 3′-terminal phosphate or phosphoester moiety, where the additional negative charge of the terminal phosphate provides for greater gel mobility than the corresponding authentic 13-nucleotide marker. Oxidative cleavage of DNA is known to result in the loss of a nucleoside, or nucleoside fragment, leaving 5′ and 3′ termini that carry a phosphate or modified phosphate residues.[33] Scission at the primary site in the 46mer self-cleaving DNA is expected to result from the oxidative removal of the A14 nucleoside, with a concomitant DNA strand break to yield a 5′ terminal product that carries the initial 13 nucleotides of the substrate (Fig. 1b). The remaining pattern is indicative of the similar cleavage of DNA linkages that are mainly located on the 3′ side of the primary cleavage site. DNA strand scission at these minor sites totals ~30% of the substrate cleavage activity, with ~70% occurring at the primary site of cleavage.

Cleavage can also be detected by autoradiography when the 5′ terminus of the catalyst strand is radiolabeled. 5′ ^{32}P-labeled c4 is found to undergo DNA cleavage at as many as five different locations with nearly equal efficiency (Fig. 7a). The shortest cleavage fragment has a gel mobility that is between that of authentic 8- and 9-nucleotide synthetic DNAs whose sequences match that of the 5′ terminus of c4. The gel mobility of the shortest DNA cleavage product is like that expected for an 8-nucleotide DNA that carries a 3′-terminal phosphate or modified phosphate residue. This cleavage site maps to nucleotide 26 of the 46mer self-cleaving DNA, and adjacent sites of DNA cleavage span nucleotides 27–30 (Fig. 1b).

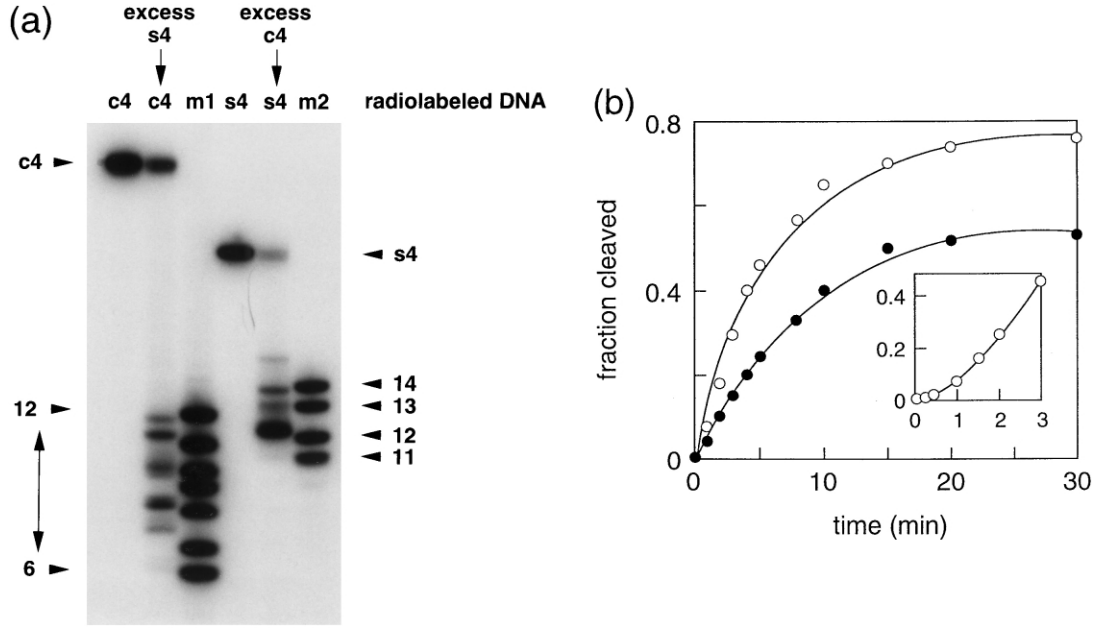

Figure 7. Examination of the DNA fragments that result from deoxyribozyme-mediated cleavage of the substrate and catalyst oligonucleotides. (a) Trace amounts of 5′ ^{32}P-labeled DNA as indicated were incubated in the absence or presence of excess (5 μM) unlableled substrate s4 or catalyst c4 DNA also as indicated. Reactions were conducted in buffer A containing 30 μM $CuCl_2$ and were incubated at 23 °C for 15 min (labeled catalyst DNA) or 30 min (labeled substrate DNA). Reaction products were separated by denaturing 20% PAGE and were visualized by autoradiography. Lanes designated m1 and m2 were loaded with 5′ ^{32}P-labeled synthetic DNAs of different lengths as indicated, each with a sequence that corresponds to the 5′ terminus of the catalyst and substrate DNAs, respectively. Numbers indicate the lengths of these radiolabeled marker DNAs. (b) Plot of the fraction s4 cleaved (open circles) and the fraction c1 cleaved (filled circles) versus time. Inset: expansion of the early part of the cleavage reaction plot for s4. Trace amounts of 5′ ^{32}P-labeled s4 or c1 were incubated for various times in the presence of 5 μM unlabeled c1 or s4, respectively. Reactions were conducted in buffer A containing 30 μM $CuCl_2$ and were incubated at 23 °C. The reaction products were separated by 20% PAGE and were quantitated by PhosphorImager.

Cleavage of the substrate DNA proceeds more rapidly than does cleavage of the catalyst DNA. In the presence of excess c1, s4 is cleaved with a combined rate constant of $\sim 0.2\,min^{-1}$ (buffer A, 30 μM $CuCl_2$), reaching a plateau of ~80% cleaved after 20 min. In contrast, combined cleavage of c1 in the presence of excess s4 proceeds with a combined rate constant of $\sim 0.1\,min^{-1}$, and reaches a cleavage maximum of ~55% (Fig. 7b). This observation is consistent with our earlier report that self-cleavage localized in the substrate domain versus self-cleavage that occurs within the catalytic core gives a ratio of ~2:1.[28]

Both the 46mer self-cleaving DNA and the bimolecular complex show reaction kinetics that vary from that expected for a pseudo-first-order process. Fig. 7b (inset) depicts a typical plot for DNA cleavage either with the unimolecular reaction, or with the bimolecular reaction when conducted with at high concentrations of substrate or enzyme. The early portion of the plot shows a distinct lag phase, thereby complicating the determination of initial rates of DNA cleavage. This lag phase is most likely indicative of a slow folding step or a necessary chemical step that is preliminary to DNA chain cleavage. In order to minimize the influence of this lag phase on rate determinations, we excluded data points that were collected during the lag phase.

The cleavage sites in the substrate oligonucleotide were also mapped by internally labeling the substrate DNA at different phosphates near the sites of cleavage. The 12-nucleotide primer oligonucleotide (corresponding in sequence to the 5′ portion of s1) was extended on a DNA template with reverse transcriptase and different [α-^{32}P]-labeled deoxynucleotide triphosphates to produce substrate DNAs that carry a radioactive phosphorus atom at defined internucleotide linkages (Fig. 8a). Incubation of these differently-radiolabeled s7 DNAs with the corresponding catalyst DNA (c7) yields a series of products that are indicative of the site of DNA cleavage. Specifically, the s7 DNA substrates that carry a ^{32}P-labeled phosphate immediately 5′ to either G13 or A14 (s7G and s7A) were cleaved by c7 to produce only 5′-cleavage fragments that carry a labeled phosphate moiety. In contrast, s7T carries a labeled phosphate immediately 5′ to T15 and only yields ^{32}P-labeled product that corresponds to the 3′-cleavage fragment. As expected, the 5′-radiolabeled substrate and product migrate faster during PAGE than do the internally labeled DNAs that lack the 5′-phosphate group. From this data, we conclude that s7 is cleaved between phosphates that are immediately 5′ to A14 and T15, and that no phosphate moieties are eliminated from the DNA molecules upon chain cleavage.

The chemical composition of the substrate 5′-cleavage fragment was examined in greater detail using several enzymatic reaction assays. First, we examined whether the 13-nucleotide cleavage product (5′-cleavage fragment derived from an s4/c4 cleavage reaction) could be annealed to a complementary template DNA and subsequently extended by reverse transcriptase. We find that the 5′-cleavage fragment cannot be extended by

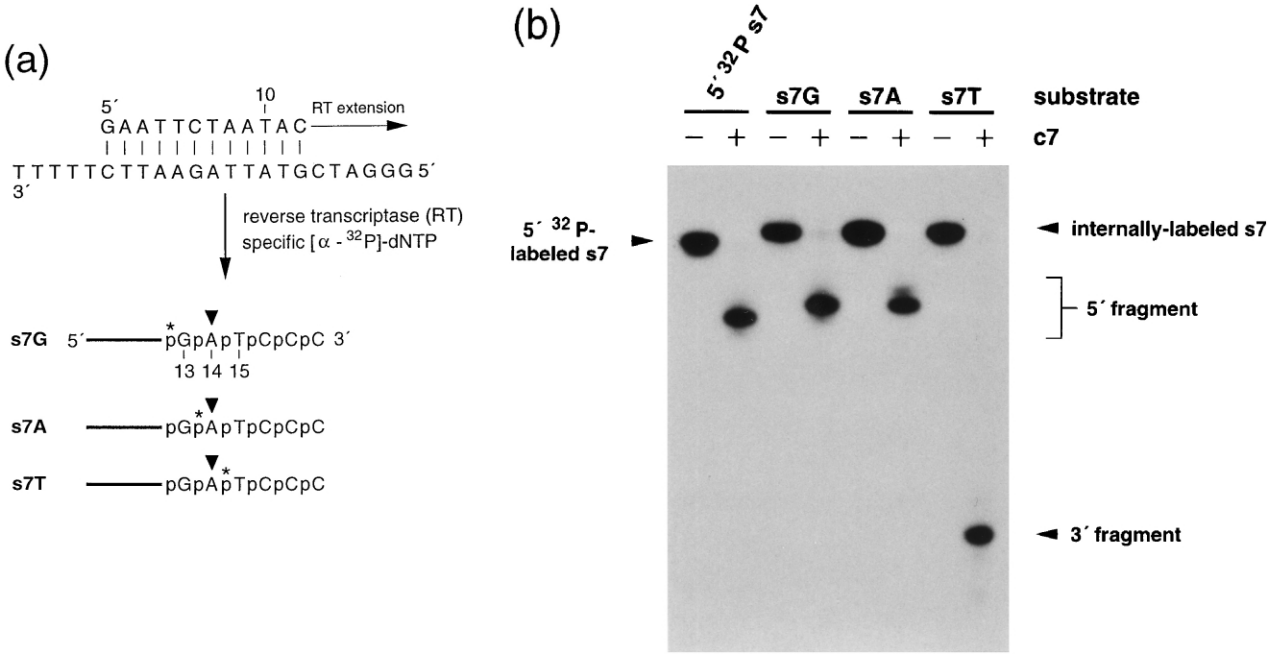

Figure 8. Cleavage site analysis using internally labeled substrate DNAs. (a) A 12-nucleotide DNA oligonucleotide corresponding in sequence to the 5′ side of the cleavage site was extended on a template DNA by reverse transcriptase (RT) in the presence a dNTP mixture of which one type was [α-^{32}P]-labeled. The full-length substrates s7G, s7A, and s7T were prepared using [α-^{32}P]-labeled GTP, ATP or TTP, respectively, and were purified by denaturing 20% PAGE prior to use. Asterisks identify the ^{32}P-labeled phosphates and the filled triangles identify the putative major site of DNA cleavage. Numbers correspond to nucleotides in the substrate DNA, beginning with the 5′-terminal nucleotide. (b) c7-mediated cleavage of various ^{32}P-labeled s7 DNAs. The substrate '5′ ^{32}P s7' was prepared by primer extension of 5′ ^{32}P-labeled 12mer using reverse transcriptase. A trace amount of 5′ ^{32}P s7 was incubated with thermocycling as described previously[29] in the absence (−) or presence (+) of 5 μM c7. Likewise, the internally labeled substrates were incubated with excess c7, and the reaction products for each were separated by denaturing 20% PAGE and imaged by autoradiography.

reverse transcriptase, while the authentic 12-nucleotide DNA can be efficiently extended (Fig. 9). Moreover, incubation of the 12-nucleotide DNA with Klenow enzyme in the absence of template DNA or dNTPs results in the degradation of the 5′ ^{32}P-labeled DNA, due to the 3′,5′-exonuclease activity of the polymerase enzyme.[44,45] In contrast, the 5′-cleavage fragment is resistant to the exonuclease activity of the Klenow enzyme, indicating that the 3′ terminus of the DNA cleavage product carries a chemical moiety that blocks the exonuclease activity. Enzymatic dephosporylation with calf intestinal phosphatase was found to convert only a small portion of the 5′-cleavage fragment into a product that was susceptible to the nuclease activity of the Klenow enzyme (data not shown). This finding is consistent with the possibility that DNA cleavage at the primary target site results in the formation of a DNA fragment that carries a 3′-terminal modified phosphate group.

Further analysis of the products resulting from c7-mediated cleavage of s7A and s7T was carried out to more accurately define the chemical composition of each cleavage fragment. In the absence of thermocycling, the c7-mediated cleavage of s7A yields three distinct products (Fig. 10a, products 1–3 of lane 3) that are differentially susceptible to the action of phosphatase. Specifically, DNA in band 1 is most likely comprised of the 5′ 13 nucleotides of s7, which is terminated with a modified (and ^{32}P-labeled) phosphate group (Figs 8 and 9). This is the product that is expected to result from the oxidative attack at nucleotide 14 of the substrate. Therefore, the cleavage fragments that are present in bands 2 and 3 most likely result from cleavage at T15, wherein the radiolabeled phosphorus atom resides in the penultimate phosphate group. Phosphatase treatment has no significant effect on the gel mobility or the relative intensity of band 1 (Fig. 10a, compare lanes 3 and 4), although a small amount of inorganic phosphate is generated during the enzymatic digest. This finding is consistent with the previous observation that only a small amount of this major cleavage product is susceptible to degradation by the Klenow enzyme after treatment with phosphatase (Fig. 9). The 5′ DNA fragment resulting from cleavage at the major site most likely carries a 3′-terminal phosphate group that retains some portion of the oxidized A14 nucleotide (Fig. 10b).

In contrast, the majority of the DNA molecules in band 2 are susceptible to the action of phosphatase. Since the radiolabeled phosphate is predicted to be at the penultimate position, removal of the 3′-terminal phosphate is not expected to produce radiolabeled inorganic phosphate. Rather, phosphatase-treated DNAs from band 2 appear to have slower gel mobility (due to removal of the negatively charged phosphate group) and add to the relative intensity of band 3. This data is consistent with the view that band 2 is comprised of different DNAs that have either a modified or an unmodified phosphate group at the 3′ terminus (Fig. 10b). The apparent identical gel mobilities of the dephosphorylated DNAs from band 2 and the DNAs present in band 3 suggest that these DNAs are identical in composition. Consistent

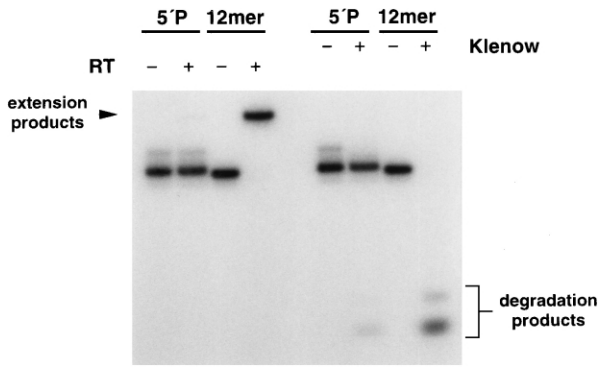

Figure 9. Analysis of the chemical structure of the s4 substrate's 5′-cleavage fragment using polymerase enzymes. 5′ ^{32}P-labeled cleavage fragment (5′P; 13-nucleotides) or a 5′ ^{32}P-labeled 12-nucleotide synthetic DNA (12mer) were incubated in a template-directed extension reaction (− or + RT) or in a depolymerization reaction (− or + Klenow enzyme) and the products were analyzed by denaturing 20% PAGE.

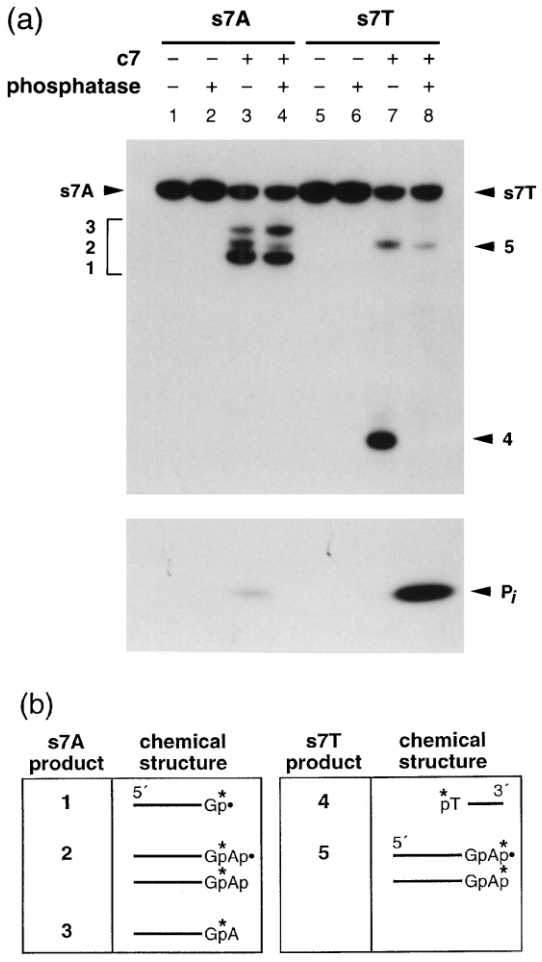

Figure 10. Examination of cleavage fragment termini using alkaline phosphatase. (a) Internally ^{32}P-labeled oligonucleotides s7A or s7T as denoted were incubated in the absence (−) or presence (+) of c7 deoxyribozyme. The resulting DNAs were separated by denaturing 20% PAGE either without (−) or with (+) pretreatment with phosphatase. DNA cleavage products 1–5 are identified accordingly. P_i denotes inorganic phosphate. A portion of the autoradiogram corresponding to the gel mobility of oligonucleotides spanning one- to four-nucleotides has been removed to reduce the size of the image. (**b**) Chemical composition of cleavage fragment termini. Asterisks identify ^{32}P-labeled phosphate groups. Filled circles represent nucleotide fragments that block the action of alkaline phosphatase.

with this possibility is the fact that band 3 DNAs are resistant to the action of phosphatase. We speculate that the DNA fragments found in bands 2 and 3 are the result of oxidative attack at T15, where the subsequent chemical rearrangements that lead to DNA chain cleavage can proceed via several different degradative pathways and yield several distinct chemical structures.

Similarly, we examined the radiolabeled cleavage products resulting from c7-mediated cleavage of s7T. Two radiolabeled product bands (Fig. 10a, bands 4 and 5 of lane 7) are generated. Band 4 presumably is the 3′ fragment that results upon attack at the major cleavage site. This product is entirely dephosphorylated during the phosphatase treatment (Fig. 10a, compare lanes 7 and 8), demonstrating that oxidative cleavage at A14 yields an unmodified phosphate group at the 5′ terminus of the 3′-cleavage fragment (Fig. 10b). Band 5 is expected to be identical in composition to band 2, except that the radiolabeled phosphate is located at the last position, as opposed to the penultimate position. Indeed, treatment with phosphatase results in partial loss of band 5 like that seen with band 2. However, the dephosphorylated products do not shift to a new band, but are no longer visible due to the loss of the radiolabeled phosphate group. A summary of the radiolabeled cleavage products that are predicted by the results described above is given in Fig. 10b.

(a)

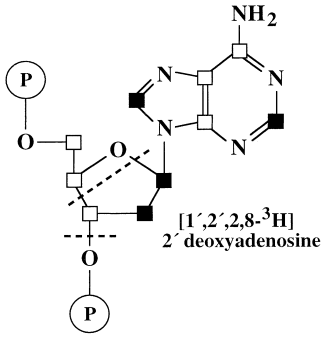

(b)

DNA	replicate 1	2	3	average
s7	1.036	0.991	0.989	1
12mer	0.039	0.033	0.021	0.031
s7 (uncleaved)	0.901	0.982	0.983	0.955
band 1	0.042	0.039	0.027	0.036
band 2	0.888	0.976	0.847	0.904

Figure 11. Oxidative destruction of the target site nucleotide. (a) Chemical structure of 2′-deoxyadenosine within the context of a DNA oligonucleotide. Open and filled squares identify hydrogenated and tritiated carbon atoms, respectively. Dashed lines depict possible locations of nucleoside fragmentation mediated by deoxyribozyme action. (b) $^{3}H/^{32}P$ ratios of double-labeled s7 (5′ ^{32}P; ^{3}H A14), single-labeled 12mer (5′ ^{32}P-GAATTCTAATAC), and the products resulting from double-labeled s7 treatment with c7 deoxyribozyme. Uncleaved s7, band 1, and band 2 are as identified in lane 3 of Fig. 10(a). The $^{3}H/^{32}P$ ratios, given for three replicate experiments, were established by excising the appropriate band after denaturing 20% PAGE, eluting the DNA from the gel, and quantitating the amount of ^{32}P and ^{3}H by liquid scintillation counting.

The DNA cleavage mechanism was further explored by using a double-labeled (^{32}P, ^{3}H) DNA substrate to more clearly establish the fate of A14 upon cleavage at the major site. A double-labeled s7 DNA was generated that carries a 5′ ^{32}P-labeled phosphate group and a [1′,2′,2,8-^{3}H]-labeled A14 moiety (Fig. 11a), such that the specific activities of ^{32}P and ^{3}H were equal (see Experimental). Successful preparation of double-labeled s7 was confirmed by liquid scintillation counting, which gave a $^{3}H/^{32}P$ ratio of 1, whereas the 5′ ^{32}P-labeled 12mer (pre-substrate) gave a ratio of 0.031 (Fig. 11b). Double-labeled s7 was incubated with c7 and the products were separated by PAGE (analogous to that seen in lane 3 of Fig. 10a). Like untreated s7, the substrate that remained uncleaved during incubation with c7 gave a $^{3}H/^{32}P$ ratio of 1. In contrast, product bands 1 and 2 gave $^{3}H/^{32}P$ ratios of 0.036 and 0.904, respectively. These results indicate that cleavage at the major site results in loss of the ^{3}H-labeled portion of A14, while this same nucleotide remains intact when cleavage occurs at T15. Taken together, these data indicate that cleavage at A14 proceeds via a mechanism that involves oxidation of its 4′ carbon,[33] with fragmentation of the target deoxyribose moiety as depicted in Fig. 11a.

Discussion

Defining generalized requirements for the sequence and secondary structure for class II deoxyribozymes

In this study, we provide additional evidence for the secondary-structure model of a small DNA-cleaving deoxyribozyme that was isolated by using in vitro selection. During the in vitro selection process, the base identity of 20 nucleotides remain largely unchanged from the original class II self-cleaving DNA studied previously.[28] Mutations within this conserved-sequence domain result in dramatic or even complete loss of catalytic function, although we have identified a number of examples of sub-optimal DNAs where this sequence differs considerably (e.g. Fig. 5).

In addition, we find important sequence elements that reside 5′ relative to the major cleavage site. For example, deletion of the three nucleotides at the 5′-terminus of the substrate domain causes a significant drop in DNA cleavage activity (Fig. 4c). However, the 5′-terminal GAA sequence is critical only for certain constructs, as these nucleotides can be eliminated with no loss of activity if the triplex domain is strengthened by additional base-triple interactions.[29] We speculate that the triplex domain of the 46mer gains stability when the GAA leader sequence is present, perhaps through contacts made with the highly-conserved TTT loop sequence of stem II.

Like most other deoxyribozymes and ribozymes, this catalytic DNA makes extensive use of conventional base-pairing interactions for substrate binding and structural folding. We have identified two stem structures within the minimized class II deoxyribozyme using mutagenesis analysis. With one exception, the base

identities of the paired nucleotides of stem I are not important as long as base complementation is maintained. Changing the G13–C27 base pair (Fig. 1a) to a C–G pair greatly reduces the rate of substrate cleavage (data not shown). This class of DNA-cleaving deoxyribozymes is unique in its use of stem II to form a triplex structure with the substrate domain. As a result, the pistol-like secondary structure for class II DNAs differs significantly from the more conventional secondary structures of RNA-cleaving deoxyribozymes.[11–18]

Products of class II deoxyribozyme-mediated DNA cleavage

DNA cleavage by class II deoxyribozymes can occur at several different positions along the polynucleotide chain, resulting in the formation of heterogeneous products. This is similar to the results of most hydroxyl radical-mediated cleavage reactions, which reflects the fact that the reactive species can diffuse from its point of origin to cleave DNA at various nearby locations.[46] Both strands of the bimolecular complexes used in this study are susceptible to oxidative cleavage. As a result, DNAs that form the bimolecular complex do not conform to the accepted definitions for 'substrate' and 'catalyst'. However, we have determined that, barring inactivation by cleavage within the catalyst domain, class II deoxyribozymes can promote more than one DNA-cleavage event. Specifically, a unimolecular structure that undergoes self-cleavage within the substrate domain can be purified and used to promote the cleavage of separate substrate DNAs that are supplied in a new reaction mixture (data not shown).

The characteristics of the deoxyribozyme reaction and the nature of the DNA cleavage products are in many ways consistent with a catalytic mechanism that involves the oxidative modification of deoxyribose. Enzymatic removal of H_2O_2 by catalase completely inhibits DNA self-cleavage. In addition, we find that supplementing the deoxyribozyme reaction mixture with H_2O_2 accelerates DNA cleavage, and can restore activity to a defective class II DNA (Fig. 2b). Both L-ascorbate and D-isoascorbic acid can restore activity to this same defective deoxyribozyme, with each having an equal effect on the reaction. Considering the lack of selectivity between the two isoforms of ascorbate, class II deoxyribozymes are not likely to form a precise binding site for this reducing agent.

The 5′ fragment produced upon DNA cleavage at the primary site has an electrophoretic mobility that is distinct from those of synthetic DNA markers, and therefore its 3′ oxygen is most likely linked to another chemical moiety (Fig. 7a). Indirect evidence indicates that this DNA cleavage product carries a 3′-terminal modified phosphate, thereby preventing both reverse transcriptase-mediated DNA extension and 3′ to 5′ exonuclease activity by the Klenow fragment (Figs 9 and 10). Hydroxyl radical attack at the 4′ carbon is known to result in the production of 5′- and 3′-cleavage products that carry a modified 3′ phosphate and an unmodified 5′ phosphate, respectively.[33] The results obtained with alkaline phosphatase treatment of cleavage products (Fig. 10) and with a double-radiolabeled DNA substrate (Fig. 11) are consistent with this predicted cleavage mechanism. DNA cleavage also occurs at the nucleotide immediately 3′ relative to the major site of cleavage. Interestingly, the data indicate that DNA chain cleavage at this secondary site proceeds by several different oxidative mechanisms to yield chemically distinct cleavage products. Determination of the exact progression of oxidative DNA cleavage at this site will require further investigation.

In our initial studies, we found that DNA self-cleavage by class II deoxyribozymes was highly sensitive to the concentration of $CuCl_2$, with catalytic activity rapidly decreasing with concentrations of copper either greater than or less than 10 μM.[28] In this study, we have found that deoxyribozyme function is significantly inhibited by the addition of excess DNA, most likely due to the nonspecific binding of free Cu^{2+} to DNA. A Cu^{2+}-dependent deoxyribozyme that promotes DNA ligation also displays considerable sensitivity to the concentration of metal ion,[42] indicating that inhibition by high concentration of Cu^{2+}-binding sites could be general. These findings indicate that examples of natural DNAs that self-cleave in the presence of Cu^{2+} and ascorbate[47,48] might be artifacts of the high-affinity interaction of Cu^{2+} with DNA, coupled with the facile production of reactive oxygen species that cleaves DNA with great efficiency.

Perhaps the most interesting characteristic of class II DNAs is their ability to function in the absence of an added reducing agent. Both H_2O_2 and ascorbate enhance the catalytic activity of class II DNAs, but these compounds are not necessary for efficient DNA cleavage activity. We have yet to fully investigate whether the catalyst DNA itself might become oxidized as part of the catalytic mechanism. Oxidative modification of DNA with intercalating oxidants,[49] for example, might give precedence for this type of reaction. However, the observation that class II deoxyribozymes are capable of multiple turn over suggests that self-oxidation is unlikely.

Deoxyribozyme-mediated cleavage of DNA

The 46mer self-cleaving DNA can be divided into two molecules by eliminating the loop from stem I. Active deoxyribozymes can then be reconstituted by combining synthetic DNA fragments, which assemble via base-pairing interactions made by stem I and by base-triple interactions that form between stem II and the substrate domain. These structural domains act as recognition elements that can be engineered to create different substrate and catalyst sequence combinations (Fig. 1c). As with certain RNA-cleaving ribozymes and deoxyribozymes, this ability can be exploited to create different class II deoxyribozymes that cleave different DNA substrates with defined specificity and affinity. One can readily create different substrate sites within larger DNA oligonucleotides and then specifically target them for cleavage using the corresponding catalyst DNA.[29] Unlike most RNA-cleaving ribozymes, the primary site of cleavage in this deoxyribozyme resides within the

base-paired portion of a stem structure (Fig. 1b). Separate catalyst DNAs, however, are incapable of cleaving a double-stranded DNA target unless repetitive heating and cooling cycles are employed.[29] Thermocycling also appears to facilitate the near quantitative processing of substrates at the primary cleavage site (Fig. 8b).[29] Successive cycles of heating and cooling may enhance the performance of catalyst DNA by allowing miscleaved DNA substrate to dissociate from the previous bimolecular complex and to undergo strand sission at the primary site upon formation of a new substrate/catalyst complex. As with most other catalytic polynucleotides, the deoxyribozymes are not 'thermostable', but the heat-denatured DNA can refold upon reaching the permissive reaction temperature without permanent loss of catalytic activity.

Several significant drawbacks hinder the use of class II DNAs as artificial restriction enzymes for single-stranded DNA. First, the substrate strand contains nucleotides whose base identities are critical for catalytic activity. Therefore, the range of DNA sequences that can be cleaved is restricted thereby precluding the targeted cleavage of any DNA sequence. Second, the catalyst strand can also be cleaved during the reaction. As a result, super-stoichiometric amounts of catalyst strand are required to cleave substrate DNA to completion. Third, oxidative DNA cleavage yields some products that cannot easily be used in other molecular biology protocols due to the nucleoside fragments that are retained by some phosphate groups. Fourth, oxidative cleavage results in the loss of sequence information, as a base is destroyed during DNA strand scission.

Conclusions

Artificial enzymes made of DNA have a number of characteristics, such as chemical stability and ease of synthesis, that make them well suited for a number of practical applications. Attractive features for a next generation and more useful DNA-cleaving DNA enzyme are user-defined substrate specificity with minimal demands on the sequence of the target DNA, rapid and multiple turn-over kinetics under mild reaction conditions, and a small size to allow efficient large-scale chemical synthesis. It is clear that single-stranded DNA has considerable potential for higher-ordered folding, and that this property makes it possible to assemble catalytic DNAs that are analogous to those made of RNA or proteins.[6–10] Therefore, it is likely that the related class I self-cleaving DNAs, or perhaps an entirely different example yet to be discovered, could be made to serve as a general 'restriction enzyme' for single-stranded DNA.

Experimental

DNA oligonucleotides

Synthetic DNAs were made by standard automated chemical synthesis (Keck Biotechnology Resource Laboratory, Yale University), and were purified by denaturing (8 M urea) polyacrylamide gel electrophoresis (PAGE) prior to use. Radiolabeled DNA was prepared by enzymatically tagging the 5′ terminus of synthetic DNAs in a reaction containing 25 mM CHES (pH 9.0 at 23 °C), 5 mM $MgCl_2$, 3 mM DTT, 1 μM DNA, 1.2 μM [γ-^{32}P]-ATP (~130 μCi), and 1 U/μL T4 polynucleotide kinase, which was incubated at 37 °C for 1 h. 5′ ^{32}P-labeled DNA was isolated by denaturing PAGE, recovered from the gel matrix by crush-soaking in 10 mM Tris–HCl (pH 7.5 at 23 °C), 0.2 M NaCl, and 1 mM EDTA. The recovered DNA was concentrated by precipitation with ethanol and resuspended in deionized water (Milli-Q, Millipore). Internally ^{32}P-labeled DNA was prepared as described below.

DNA cleavage assays

DNA self-cleavage assays were conducted using trace amounts of radiolabeled precursor DNA (~100 pM) at 23 °C in buffer A [50 mM HEPES (pH 7.0 at 23 °C), 0.5 M NaCl, 0.5 M KCl] containing $CuCl_2$ as indicated for each experiment unless otherwise stated. All solutions were prepared with deionized water without regard for dissolved oxygen content. Examinations of the DNA cleavage activity of bimolecular complexes were conducted under similar conditions using concentrations of substrate and catalyst DNA as indicated for each experiment. Either the substrate or the catalyst component was 5′ ^{32}P-labeled for detection purposes. Reactions were terminated by the addition of a PAGE loading buffer (8 M urea, 5 mM Tris–borate (pH 8.3 at 23 °C), 0.3 M sucrose, 50 mM Na_2EDTA, 0.02% w/v xylene cyanol, and 0.02% w/v bromophenyl blue). Cleavage products were separated by denaturing PAGE and imaged by autoradiography or by PhosphorImager (Molecular Dynamics). Product yields were determined by quantitation of the corresponding precursor and product bands.

Reverse transcriptase and Klenow enzyme reactions

Reverse transcriptase (SuperScript II, GibcoBRL) reactions used to produce internally labeled DNA substrates were conducted in a 20-μL volume containing 50 mM Tris–HCl (pH 8.3 at 23 °C), 75 mM KCl, 3 mM $MgCl_2$, 1 mM dithiothreitol, 0.2 mM each of the three appropriate unlabeled dNTPs, 2 μM (~120 μCi) of the appropriate [α-^{32}P]-dNTP, and 10 U/μL reverse transcriptase. After incubating the reactions at 37 °C for 30 min, the internally labeled DNAs were purified by denaturing 20% PAGE and isolated from the matrix as described previously. Double-labeled s7 DNA was prepared in a 100-μL reaction containing 0.5 μM 5′ ^{32}P-labeled 12mer DNA, 1 μM template DNA in addition to the reagents listed above, except that [1′,2′,2,8,3H] dATP (~10 μCi; Amersham) was used in place of unlabeled dATP. The chemical nature of the 3′ terminus of the 5′ cleavage fragment of s1 was examined by incubating 5′ ^{32}P-labeled s1/c1 cleavage product in the presence of either reverse transcriptase or Klenow enzyme. 5′ ^{32}P-labeled fragment was isolated by denaturing 20% PAGE from a deoxyribozyme cleavage reaction containing ~0.1 μM 5′

^{32}P-labeled s1, 5 μM c1, 30 μM $CuCl_2$ in a total volume of 100 μL buffer A. Extension reactions were conducted in the presence or absence of reverse transcriptase as described above, except that 0.2 mM of each unlabeled dNTP was used. In addition, the reverse transcriptase extension reactions contained 2 μM of the DNA template 5′-GGAGTCGTATTAGAATTC. Klenow enzyme reactions were conducted in the presence of 50 mM Tris–HCl (pH 7.5 at 23 °C), 10 mM $MgCl_2$, 1 mM DTT, 50 μg/mL BSA, and were incubated in the presence or absence of 0.5 U/μL Klenow enzyme at 37 °C for 30 min.

Phosphatase treatment of internally labeled DNA substrates

Treatment of DNA cleavage fragments with alkaline phosphatase was carried out in the presence of 50 mM Tris–HCl (pH 8.5 at 23 °C), 0.1 mM EDTA and 0.05 U/μM calf intestinal alkaline phosphatase (Boehringer Mannheim). Each alkaline phosphatase reaction was incubated at 37 °C for 1 h. Radiolabeled DNA cleavage products were supplied to the reaction by the addition of 2 μL of a 20-μL deoxyribozyme reaction containing 50 mM HEPES (pH 7.0 at 23 °C), 0.5 M NaCl, 30 μM $CuCl_2$, 5 μM c7 and trace amounts of internally labeled s7A or s7T that was incubated for 20 min.

Acknowledgements

We thank members of the Breaker laboratory for helpful discussions. This work was supported by a Young Investigator Award to R.R.B. from the Arnold and Mabel Beckman Foundation.

References

1. Gold, L.; Polisky, B.; Uhlenbeck, O.; Yarus, M. *Annu. Rev. Biochem.* **1995**, *64*, 763.
2. Breaker, R. R. *Curr. Opin. Chem. Biol.* **1997**, *1*, 26.
3. Osborne, S. E.; Ellington, A. D. *Chem. Rev.* **1997**, *97*, 349.
4. Hermann, T.; Patel, D. J. *Science* **2000**, *287*, 820.
5. Burgstaller, P.; Famulok, M. *Angew. Chem., Int. Ed. Engl.* **1995**, *34*, 1189.
6. Breaker, R. R. *Nat. Biotechnol.* **1997**, *15*, 427.
7. Li, Y.; Breaker, R. R. *Curr. Opin. Struct. Biol.* **1999**, *9*, 315.
8. Sen, D.; Geyer, C. R. *Curr. Opin. Chem. Biol.* **1998**, *2*, 680.
9. Breaker, R. R. *Nat. Biotechnol.* **1999**, *17*, 422.
10. Breaker, R. R. *Chem. Rev.* **1997**, *97*, 371.
11. Breaker, R. R.; Joyce, G. F. *Chem. Biol.* **1994**, *1*, 223.
12. Breaker, R. R.; Joyce, G. F. *Chem. Biol.* **1995**, *2*, 655.
13. Faulhammer, D.; Famulok, M. *Angew. Chem., Int. Ed. Engl.* **1996**, *35*, 2837.
14. Geyer, C. R.; Sen, D. *Chem. Biol.* **1997**, *4*, 579.
15. Faulhammer, D.; Famulok, M. *J. Mol. Biol.* **1997**, *269*, 188.
16. Roth, A.; Breaker, R. R. *Proc. Natl. Acad. Sci. U.S.A.* **1998**, *95*, 6027.
17. Santoro, S. W.; Joyce, G. F. *Proc. Natl. Acad. Sci. U.S.A.* **1997**, *94*, 4262.
18. Li, J.; Zheng, W.; Kwon, A. H.; Lu, Y. *Nucleic Acids Res.* **2000**, *28*, 481.
19. Dash, B. C.; Harikrishnan, T. A.; Goila, R.; Shahi, S.; Unwalla, H.; Husain, S.; Banerjea, A. C. *FEBS Lett.* **1998**, *431*, 395.
21. Warashina, M.; Kuwabara, T.; Nakamatsu, Y.; Taira, K. *Chem. Biol.* **1999**, *6*, 237.
22. Cairns, M. J.; Hopkins, T. M.; Witherington, C.; Wang, L.; Sun, L.-Q. *Nat. Biotechnol.* **1999**, *17*, 480.
23. Santiago, F. S.; Lowe, H. C.; Kavurma, M. M.; Chesterman, C. N.; Baker, A.; Atkins, D. G.; Khachigian, L. M. *Nat. Med.* **1999**, *5*, 1264.
24. Wu, Y.; Yu, L.; McMahon, R.; Rossi, J. J.; Forman, S. J.; Snyder, D. S. *Hum. Gene Ther.* **1999**, *10*, 2847.
25. Yen, L.; Strittmatter, S. M.; Kalb, R. G. *Ann. Neurol.* **1999**, *46*, 366.
26. Li, Y.; Breaker, R. R. *J. Am. Chem. Soc.* **1999**, *121*, 5364.
27. Sheppard, T. L.; Ordoukhanian, P.; Joyce, G. F. *Proc. Natl. Acad. Sci. U.S.A.* **2000**, *97*, 7802.
28. Carmi, N.; Shultz, L. A.; Breaker, R. R. *Chem. Biol.* **1996**, *3*, 1039.
29. Carmi, N.; Balkhi, S. A.; Breaker, R. R. *Proc. Natl. Acad. Sci. U.S.A.* **1998**, *95*, 2233.
30. Buettner, G. R.; Jurkiewicz, B. A. *Radiat. Res.* **1996**, *145*, 532.
31. Chiou, S.-H. *J. Biochem.* **1983**, *94*, 1259.
32. Halliwell, B.; Aruoma, O. I. *FEBS Lett.* **1991**, *281*, 9.
33. Joshi, R. R.; Likhite, S. M.; Kumar, R. K.; Ganesh, K. N. *Biochim. Biophys. Acta* **1994**, *1199*, 285.
34. Veal, J. M.; Merchant, K.; Rill, R. L. *Nucleic Acids Res.* **1991**, *19*, 3383.
35. Sigman, D. S.; Mazumder, A.; Perrin, D. M. *Chem. Rev.* **1993**, *93*, 2295.
36. Hirao, I.; Kawai, G.; Yoshizawa, S.; Nishimura, Y.; Ishido, Y.; Watanabe, K.; Miura, K. *Nucleic Acids Res.* **1994**, *22*, 576.
37. Mirkin, S. M.; Frank-Kamenetskii, M. D. *Annu. Rev. Biophys. Biomol. Struct.* **1994**, *23*, 541.
38. Moser, H. E.; Dervan, P. B. *Science* **1987**, *238*, 645.
39. Clauwaert, J.; Stockx, J. *Z. Naturforsch. B* **1968**, *23*, 25.
40. Saenger, W. In *Principles of Nucleic Acid Structure* Springer-Verlag: New York, 1984 pp 105–115.
41. Lavelle, L.; Fresco, J. R. *Nucleic Acids Res.* **1995**, *23*, 2692.
42. Cuenoud, B.; Szostak, J. W. *Nature* **1995**, *375*, 611.
43. Rifkind, J. M.; Shin, Y. A.; Heim, J. M.; Eichhorn, G. L. *Biopolymers* **1976**, *15*, 1879.
44. Klenow, H.; Henningsen, I. *Proc. Natl. Acad. Sci. U.S.A.* **1997**, *65*, 168.
45. Joyce, C. M.; Grindley, N. D. F. *Proc. Natl. Acad. Sci. U.S.A.* **1983**, *80*, 1830.
46. Hermann, T.; Heumann, H. *RNA* **1995**, *1*, 1009.
47. Kazakov, S. A.; Astashkina, T. G.; Mamaev, S. V.; Vlassov, V. V. *Nature* **1988**, *335*, 186.
48. Wang, Y.; Van Ness, B. *Nucleic Acids Res.* **1989**, *17*, 6914.
49. Hall, D. B.; Holmlin, R. E.; Barton, J. K. *Science* **1996**, *382*, 731.